Published in final edited form as:
Biochim Biophys Acta. 2014 September ; 1842(9): 1596–1603. doi:10.1016/j.bbadis.2014.05.016.

Mutant LRRK2 Enhances Glutamatergic Synapse Activity and Evokes Excitotoxic Dendrite Degeneration

Edward D. Plowey[a,g], **Jon W. Johnson**[c,d,i], **Erin Steer**[a], **Wan Zhu**[g], **David A. Eisenberg**[c], **Natalie M. Valentino**[c], **Yong-Jian Liu**[f], and **Charleen T. Chu**[a,b,e,h,i]

[a]Department of Pathology, University of Pittsburgh, Pittsburgh, PA

[b]Department of Ophthalmology, University of Pittsburgh, Pittsburgh, PA

[c]Department of Neuroscience, University of Pittsburgh, Pittsburgh, PA

[d]Department of Psychiatry, University of Pittsburgh, Pittsburgh, PA

[e]McGowan Institute for Regenerative Medicine, University of Pittsburgh, Pittsburgh, PA

[f]Department of Physiology, Nanjing Medical University, Nanjing, China

[g]Department of Pathology, Stanford University, Stanford, CA

[h]Pittsburgh Institute for Neurodegenerative Diseases, University of Pittsburgh, Pittsburgh, PA

[i]Center for Neuroscience, University of Pittsburgh, Pittsburgh, PA

Abstract

Mutations in leucine rich repeat kinase 2 (LRRK2), which are associated with autosomal dominant Parkinson's disease, elicit progressive dendrite degeneration in neurons. We hypothesized that synaptic dysregulation contributes to mutant LRRK2-induced dendritic injury. We performed *in vitro* whole-cell voltage clamp studies of glutamatergic receptor agonist responses and glutamatergic synaptic activity in cultured rat cortical neurons expressing full-length wild-type and mutant forms of LRRK2. Expression of the pathogenic G2019S or R1441C LRRK2 mutants resulted in larger whole-cell current responses to direct application of AMPA and NMDA receptor agonists. In addition, mutant LRRK2-expressing neurons exhibited an increased frequency of spontaneous miniature excitatory postsynaptic currents (mEPSCs) in conjunction with increased excitatory synapse density as assessed by immunofluorescence for PSD95 and VGLUT1. Mutant LRRK2-expressing neurons showed enhanced vulnerability to acute synaptic glutamate stress. Furthermore, treatment with the NMDA receptor antagonist memantine significantly protected against subsequent losses in dendrite length and branching complexity. These data demonstrate an

Corresponding Author: Charleen T. Chu, MD, PhD, Department of Pathology, University of Pittsburgh School of Medicine, 3550 Terrace Street, Pittsburgh, PA 15213, ctc4@pitt.edu.

Conflict of Interest Statement
The authors have no conflicts of interest.

early association between mutant LRRK2 and increased excitatory synapse activity, implicating an excitotoxic contribution to mutant LRRK2 induced dendrite degeneration.

Keywords

LRRK2; excitotoxicity; calcium; neurodegeneration

Introduction

Parkinson's disease (PD) is a progressive neurodegenerative disorder characterized by debilitating motor, and in many cases cognitive, deficits. Efforts to understand the pathogenesis of PD have revealed genetic factors that increase the risk for developing PD. Leucine-rich repeat kinase 2 (LRRK2) mutations underlie *PARK8*-linked familial parkinsonism [1, 2]. This protein is believed to play important roles in both familial and sporadic PD pathogenesis [3]. A deeper understanding of the pathologic cascade that leads to neurodegeneration downstream of mutant LRRK2 will likely render novel insights for the prevention and treatment of PD.

Neurite injury is a conspicuous feature of mutant LRRK2-associated neurodegeneration. Mutant LRRK2 expression in SH-SY5Y neuroblastoma cell line cultures and in mouse primary cortical neurons is associated with neurite degeneration [4] or reduced dendrite outgrowth [5, 6]. Mutant LRRK2 expression in neurons *in vivo* or *in vitro* results in neurite injury that precedes cell death [7]. Functional neurotransmission abnormalities [8] and dystrophic neurite morphology have been reported in transgenic mutant LRRK2 mice [9, 10]. Whereas numerous effector pathways, including autophagy [7, 10–13], mitochondrial pathology [14–16], calcium toxicity [15], the ubiquitin proteasome [17], microtubule stability [18], growth cone dynamics [6, 19], Fas-associated protein with death domain [20] and Rac1 [21], have been proposed, less is known about possible upstream impacts of LRRK2 on synaptic function [22–25]. We hypothesize that synaptic dysregulation contributes to dendrite injury in mutant LRRK2 expressing neurons.

To test our hypothesis, we determined whether alterations in excitatory synapses underlie neurite retraction in neurons expressing PD-associated LRRK2 mutations. We found that mutant LRRK2-expressing neurons show evidence of increased glutamatergic synapses and increased vulnerability to synaptic glutamate stress, which occur well before the onset of neurite degeneration. Furthermore, the NMDA receptor antagonist memantine partially protected neurons from mutant LRRK2-induced dendrite degeneration. These findings suggest that mutant LRRK2 is associated with enhanced glutamatergic synapses and renders neurons more vulnerable to glutamate receptor toxicity.

Materials and Methods

Neuronal Cultures

Timed-pregnant female Sprague-Dawley rats (E16), obtained from Hilltop Lab Animals, Inc. (Scottsdale, PA), were euthanized by CO_2 inhalation. This method of euthanasia is consistent with methods suggested by the Panel on Euthanasia of the American Veterinary

Medical Association to minimize animal distress and was approved by the University of Pittsburgh Institutional Animal Care and Use Committee (IACUC). Embryos of either gender were harvested in ice-cold Hanks solution (Invitrogen). Cerebral cortices were dissected and dissociated via trypsinization and gentle pipette trituration. Cell suspensions were plated at a density of 100,000 cells/cm^2 onto glass cover slips (Carolina Biological) or plastic culture dishes coated with poly-D-lysine (0.1 mg/ml; Sigma) and laminin (5 μg/ml; Roche Diagnostics). Cultures were maintained at 37°C with 5% ambient CO_2 in Neurobasal medium (Invitrogen) supplemented with B27 (Invitrogen) and 1% Glutamax-I (Invitrogen). Media refreshments were performed every other day. In some experiments, memantine, an NMDA receptor antagonist, was added to the culture media following neuronal transfection to maintain a concentration of 1 μM.

Molecular Constructs and Culture Transfection

Full-length wild-type (WT) and mutant LRRK2 cDNAs (pathogenic PD mutations G2019S or R1441C; kinase impaired K1906M) with C-terminal triple-hemagluttinin tags (LRRK2-3HA) were expressed via the pcDNA3.1 vector [11]. Neuronal cultures were co-transfected with pRK7-eGFP and either empty pcDNA3.1 vector or mutant LRRK2 cDNA constructs with 0.1% Lipofectamine 2000 reagent (Invitrogen) on days *in vitro* (DIV) 12–15. A molar ratio of 1:2 (eGFP:LRRK2-3HA) was employed in electrophysiology experiments, which yields 85% co-expression (Supplementary Fig. S1F-G), and ratios of 1:2 and 1:9 were used in immunofluorescence experiments. A mouse anti-HA Tag IgG (Covance, Clone 16B12) was used to confirm LRRK2-3HA protein expression in neuroblastoma cells via western blot (1:1000 primary antibody dilution) and in cultured cortical neurons via immunocytochemistry (1:100 primary antibody dilution). RT-PCR was performed on neuronal cultures with primers spanning the junction of the C-terminus and the 3HA tag of the LRRK2 cDNAs (LRRK2-3HA primer sequences (403 base pair product): LRRK2-7179-Forward: 5’-AAGGGAGGTAATGGTAAAAGAAA-3’ ; LRRK2-3HA-Reverse: 5’-CCGCCCTCAACAGATGTTCG-3’; eGFP primer sequences (402 base pair product): eGFP-Forward: 5’-GAGCTGGACGGCGACGTAAACGG-3’; eGFP-Reverse: R: 5’-GACGTTGTGGCTGTTGTAGTTG-3’). The transfection efficiency, determined by GFP fluorescence and HA Tag immunofluorescence, was less than 1% (40–75 neurons per cover slip). There was typically one transfected neuron in a medium-power (100X) microscopic field, allowing us to focus our analysis on the postsynaptic effects of mutant LRRK2 expression in individual neurons in the context of non-transfected presynaptic terminals from surrounding neurons.

Electrophysiological Recordings

Cover slips containing rat primary cortical neuron cultures were placed in a recording chamber containing Ringer solution (140 mM NaCl, 2.8 mM KCl, 1 mM $CaCl_2$, 10 mM HEPES, 10 mM glucose; pH 7.3) with tetrodotoxin (2 μM) and strychnine (1 μM). Transfected cells expressing GFP were visualized via epifluorescence microscopy. Whole-cell voltage clamp recordings (Axopatch 200 Amplifier) were obtained with glass micropipettes (tip resistance 3–5 MΩ) filled with intracellular solution (130 mM CsCl, 10 mM HEPES, 10 mM EGTA for glutamate receptor agonist responses and 118 mM Cs Methane Sulfonate, 12 mM CsCl, 10 mM HEPES, 10 mM EGTA for mEPSC recordings).

The mean +/- SEM series resistance was 16.1 ± 0.8 MΩ and was compensated at 80% in all experiments. Holding potentials were −55 mV for agonist responses and −60 mV in mEPSC recordings (corrected for liquid junction potentials of 5 and −10 mV, respectively). Cells were exposed to ionotropic glutamate receptor agonists (100 μM AMPA or 10 μM NMDA/10 μM glycine for 20 second periods) through a gravity-driven, multi-barrel fast perfusion system [26]. NMDA receptor currents were inhibited during applications of AMPA with 1 mM $MgCl_2$. Data were digitized (Digidata 1200) and recorded to a PC running pClamp 9.1 software suite. Whole-cell current responses were quantified as the mean steady state current during the final 5 seconds of agonist applications. mEPSC mean amplitudes and frequencies were analyzed using the event detection module of pClamp 9.1.

Synaptic Protein Immunocytochemistry

Cover slips were fixed with 4% paraformaldehyde with 4% sucrose followed by 100% methanol, permeabilized with 0.1% Triton-X and blocked with Superblock Buffer (Thermo Scientific). Primary and secondary antibody concentrations employed were as follows: mouse anti-PSD-95 IgG (1:200; Neuromab 75-028, UC Davis), mouse anti-VGLUT1 IgG (1:200; Neuromab 75-066, UC Davis), rabbit anti-LRRK2 antibody (1:50; MJFF2 [c41-2], Abcam ab133474), Alexa Fluor 594-conjugated donkey-anti-mouse and goat-anti-rabbit IgGs (1:1000; Jackson ImmunoResearch Laboratories). Nuclei were counterstained with DAPI (1:500; Invitrogen). Cover slips were mounted on glass slides with gelvatol and imaged on an Olympus Fluoview 1000 confocal microscope. Proximal dendrites of all consecutively encountered transfected neurons for each LRRK2 construct (25–80 per well) were imaged with a 63x magnification, 1.40 NA apochromatic lens oil immersion objective. Identical excitation and image acquisition parameters were employed for all constructs. Images were analyzed for synapse protein immunofluorescence puncta with NIH ImageJ [27]. Immunoreactive puncta were identified on 50–250 micron GFP-positive dendrite segments from each neuron with the NIH ImageJ intensity threshold function and quantified with the Analyze Particles module of NIH ImageJ with respect to puncta density (per micron of analyzed dendrite length) and puncta area. The threshold intensity for each antigen was set as the mean plus 3 standard deviations of background dendritic cytoplasm signal sampled from 5 neurons. Identical background measurements and intensity thresholds were employed in all transfection groups.

Synaptosome Preparations and Western Blots

DIV15-17 rat cortical neurons were scraped and homogenized with a 25G needle in HEPES-buffered sucrose [0.32 M sucrose, 5 mM HEPES, pH7.4] supplemented with protease inhibitor cocktail (Sigma, P8340)]. Homogenized extracts were spun at 1,000 *g* for 10 min at 4°C. Supernatant (S1) was centrifuged again at 1,000 *g* for 10 min at 4 °C and saved (S1′, whole cell lysate). S1′ was centrifuged at 10,000 *g* for 15 min for the cytosolic (S2) fraction. The pellet was washed one time with 1 ml HEPES-buffered sucrose and centrifuged again at 10,000 *g* for 15 min. The washed pellet was either lysed for western blot analysis or lysed rapidly with 1 ml ice-cold water with protease inhibitor, adjusted to 4 mM HEPES and homogenized with a 25G needle. P2 lysates were centrifuged at 25,000 g at 4 °C rendering crude synaptic vesicle fractions (S3) and lysed synaptosomal membrane fractions (P3). Lysed synaptosomal membranes were resuspended in HEPES-lysis buffer (50 mM HEPES,

pH 7.4, 2mM EDTA, 0.5% Triton X, 1 mM NaF, 1 mM Na_3VO_4 a protease inhibitor mixture) and centrifuged at 32,000 *g* for 20 min to render solubilized synaptosomal membranes (S4) and PSD-1T fractions (P4). For western blots, protein quantification was performed via the Bradford method (Bio-rad, 500-0006) using a BioTek Epoch 96-well microplate reader (BioTek, Winooski, VT, USA). Protein samples were loaded into 4–15% Tris-Glycine gels (Bio-rad, 456–1085 and 456–1086) and transferred onto PVDF membranes (Immobilon-P, Millipore, IPVH00010). Immunoblotting was performed using the following primary antibodies: rabbit anti-LRRK2 antibody (1:1000; MJFF2 [c41-2], Abcam ab133474), mouse anti-PSD95 MAGUK scaffold protein (1:1000; clone K28/43, NeuroMab 73-028, UC Davis) and mouse anti-GluN2B/NR2B glutamate receptor (1:1000; clone N59/36, NeuroMab 73–101, UC Davis). Blots were then labeled with secondary antibodies: HRP-conjugated anti-mouse IgG (GE Healthcare, NXA-931) or HRP-conjugated anti-rabbit IgG (GE Healthcare, NA934V). Immunoreactive bands were detected by exposure of x-ray film (Denville, E3018) following incubation of blots with ECL Prime chemiluminesence reagents (GE Healthcare, RPN2236).

Excitotoxicity Assay

At three days post-transfection, culture cover slips were transferred to either physiologic Ringer solution or high K^+ solution (90 mM KCl, 53 mM NaCl, 1 mM $CaCl_2$, 10 mM HEPES, 10 mM glucose; pH 7.3) for 5 minutes. Cover slips were then returned to the incubator in their previous conditioned growth medium for a period of 12 hours. Cultures were then fixed, immunostained for cleaved caspase-3 (CC3) using rabbit polyclonal IgG (Cell Signaling #9661) diluted 1:1000 followed by Cy3-conjugated anti-rabbit IgG (1:1000; Jackson ImmunoResearch) and counterstained with DAPI (1:500 dilution; Invitrogen). Viable transfected neurons (GFP-positive with neurite processes, CC3-negative, vesicular nucleus) and apoptotic transfected neurons (GFP-positive, CC3-positive, pyknotic nucleus) were quantified for each coverslip. Nuclear pyknosis always concurred with positive CC3 immunostaining. Six replicates were performed for each plasmid. Antagonists for AMPA receptors (CNQX; 25 μM) and NMDA receptors (D-APV; 50 μM) were included in a subset of cultures during and for 12 h following potassium depolarization.

Neuronal Morphology

GFP-expressing neurons were photographed using an Olympus Provis epifluorescence microscope. All transfected neurons on each coverslip (range 50–75 neurons) were analyzed. Neurite length and branch points were quantified using the NeuronJ extension of NIH ImageJ as previously described [27, 28].

Statistical analyses

Data are expressed as means ± SEM. Data from mutant and WT LRRK2-transfected neurons in electrophysiology, immunofluorescence and excitotoxicity experiments were compared with data from vector control-transfected neurons via Analyses of Variance (ANOVA) with post-hoc Dunnett's Tests (SYSTAT Version 13.00.05). $p<0.05$ was deemed statistically significant.

Results

Mutant LRRK2-expressing neurons demonstrate increased current responses to glutamate receptor agonists and increased spontaneous excitatory synaptic activity

We first recorded whole-cell current responses to specific AMPA and NMDA receptor agonists in DIV 17 cortical neurons co-transfected with eGFP and either WT or one of several forms of mutant LRRK2-3HA three days prior. Recordings were performed 3 days following transfection, a timepoint that precedes significant alterations in the dendritic lengths of G2019S and R1441C LRRK2-expressing neurons (Supplementary Figure S1A, B). LRRK2-3HA construct expression was confirmed in neuronal cultures by RT-PCR (Supplementary Figure S1C) and in B103 rat neuroblastoma cell cultures by western blot (Supplementary Figure S1D). Transfected neurons demonstrated MAP2 immunoreactivity (Supplementary Figure S1E). HA-tag expression was detected in ~85% of GFP-positive neurons transfected with WT, G2019S, R1441C, K1906M or G2019S/K1906M LRRK2 (Supplementary Figure S1F–G). Transfected neurons were visualized by epifluorescence microscopy and recorded in whole-cell voltage clamp configuration (Supplementary Figure S1H).

Inward current responses to 100 μM AMPA were larger in G2019S and R1441C LRRK2-expressing neurons compared to vector-transfected neurons (Figures 1A and B). WT LRRK2-transfected neurons showed a trend towards an increased AMPA response, whereas kinase-impaired K1906M LRRK2-transfected neurons showed no difference in the AMPA response compared to control neurons. Current responses to 10 μM NMDA were also larger in G2019S and R1441C LRRK2-transfected neurons (Figures 1C and D), but were similar to vector control responses in WT and K1906M LRRK2-transfected neurons. To determine if mutant LRRK2 impacts endogenous glutamatergic synaptic activity, we performed voltage clamp recordings of mEPSCs in cortical neurons expressing WT or mutant LRRK2 cDNAs. Mutant LRRK2-expressing neurons showed increased frequencies of mEPSC events compared to vector transfected neurons (Figure 1E, F). There were no differences in the mean mEPSC amplitudes among vector-, WT- and mutant LRRK2-transfected neurons, providing no evidence for an alteration in average synapse strength (Figure 1G).

Mutant LRRK2 expressing neurons show increased excitatory synaptic protein immunoreactivity

We performed indirect immunofluorescence labeling of excitatory postsynaptic terminals with a PSD-95 antibody at 3 days following transfection of neuronal cultures with LRRK2-3HA constructs. Transfected neurons demonstrate punctate PSD-95 labeling colocalizing with dendritic spines (Figure 2A, B). LRRK2 itself was present in dendrites and crude synaptosomal fractions, but was not enriched in dendritic spines or PSD95-enriched fractions (Supplementary Figure S2). However, G2019S and R1441C LRRK2-expressing neurons demonstrated increased dendritic PSD-95 immunoreactivity compared to vector transfected neurons (Figure 2C). Analysis of relative PSD-95 puncta sizes did not detect significant differences among the different groups (Vector: 100 ± 4%, n=51; WT 101 ± 5%, n=39; G2019S 112 ± 5%, n=48; R1441C 114 ± 5%, n=42; K1906M 102 ± 5%, n=38). To determine whether the increased postsynaptic labeling corresponded with an increase in

excitatory synaptic markers, we performed immunocytochemical labeling of the excitatory presynaptic protein VGLUT1, which also demonstrated punctate reactivity abutting or colocalizing with dendritic spines (Figure 3A, B). A higher density of VGLUT1 labeling was observed on dendrites in G2019S or R1441C LRRK2-transfected neurons, but not K1906M LRRK2-transfected neurons (Figure 3C). Expression of the double mutant G2019S/K1906M LRRK2 also had no effect on the density of VGLUT1 immunoreactive puncta (Vector: 7.38 ± 0.60 puncta per 100 μm dendrite, n=78; G2019S/K1906M LRRK2: 7.27 ± 0.51 puncta per 100 μm dendrite, n=65), indicating a requirement for LRRK2 kinase activity.

Memantine partially protects against mutant LRRK2-induced neurodegeneration

To determine if endogenous NMDA receptors contribute to mutant LRRK2-induced neurite shortening, we treated G2019S LRRK2-expressing neurons with the NMDA receptor antagonist memantine (1 μM). Neuronal cultures were transfected on DIV 14 and then treated with 1 μM memantine continuously from 1 to 9 days following transfection (DIV 15–23; Figure 4A). The blunted dendrite length associated with 9 days of 2019S LRRK2 expression was partially reversed by treatment with 1 μM memantine (Figures 4B–C), and the number of dendrite branches was completely restored with memantine treatment (Figure 4D). These results suggest that an NMDA receptor-dependent mechanism contributes to the progressive dendritic shortening and simplification observed in G2019S LRRK2-expressing neurons.

Mutant LRRK2 expression renders neurons more vulnerable to acute synaptic glutamate stress

To determine if mutant LRRK2 increases neuronal sensitivity to acute endogenous synaptic glutamate stress, we exposed transfected cortical neurons to a brief depolarizing stimulus (5 minutes of 90 mM K^+ Ringer) to evoke synaptic glutamate release. Following a post-depolarization incubation of 12 hours in conditioned growth media, cover slips were fixed and stained with an anti-cleaved caspase 3 antibody and DAPI to reveal apoptotic transfected neurons (Figure 4E). G2019S and R1441C LRRK2-expressing neurons showed higher rates of apoptosis compared to control vector-transfected neurons (Figure 4F). Blockade of AMPA and NMDA receptors with CNQX and APV resulted in protection of all neuronal culture treatment groups, demonstrating that the depolarizing stimulus induced apoptosis via glutamate receptor-dependent mechanisms (Figure 4F).

Discussion

In this study, we investigated the impact of mutant LRRK2 expression on excitatory synapses in cultured rat cortical neurons prior to the well-documented stage of progressive mutant LRRK2-induced dendrite degeneration [7]. Neurons expressing mutant LRRK2 showed increased whole-cell current responses to AMPA and NMDA receptor agonists and increased mEPSC frequencies compared to vector-transfected control neurons. We also found that cultured mutant LRRK2-transfected neurons demonstrated increased densities of VGLUT1 and PSD-95 immunoreactive puncta compared to control neurons. Mutant LRRK2-expressing neurons demonstrated an increased propensity for cell death induced by

endogenous synaptic glutamate stress. Furthermore, the NMDA receptor antagonist memantine conferred significant protection from mutant LRRK2-induced dendrite retraction, which begins 6 days after the observed electrophysiological alterations. Our data suggest that excitatory synapse dysregulation contributes to mutant LRRK2 induced neurodegeneration.

Increased mEPSC frequency could be due to either increased numbers of synapses or increased frequency of spontaneous presynaptic single-vesicle fusion. While the transfection conditions in this study allowed us to isolate the effects to postsynaptic expression of mutant LRRK2, it is possible that a retrograde trans-synaptic effect could promote spontaneous vesicle release in the untransfected presynaptic terminals. Nevertheless, several lines of evidence support a role for increased synapse density. Immunocytochemical labeling revealed increases in both PSD-95 and VGLUT1 puncta densities along the dendrites. The larger glutamatergic receptor agonist responses observed in mutant LRRK2 transfected neurons are also consistent with increased densities of excitatory synapses. As mutant LRRK2 expression had no effects on either mEPSC amplitude or PSD-95 puncta sizes, the data do not support a modulatory effect for mutant LRRK2 on global synapse strength. Rather, the data are most consistent with increased excitatory synapse numbers as an early consequence of mutant LRRK2 expression.

Our study also implicates NMDA receptor activation as a contributing factor in the subsequent dendrite degeneration observed in mutant LRRK2-expressing neurons. Memantine treatment restored dendrite branching complexity and ameliorated the dendrite retraction phenotype observed in vehicle-treated G2019S LRRK2-expressing neurons. NMDA receptors may mediate excitotoxic injury via toxic Ca^{+2}-mediated overactivation of neuronal enzymatic processes. While the potential toxicity of synaptic NMDA receptor activation is controversial [29–31], extrasynaptic NMDA receptors may also contribute to neurotoxicity by inhibiting protective signaling cascades and activating toxic signaling pathways [32, 33]. The ability of memantine [34], to protect against mutant LRRK2-induced dendrite degeneration is consistent with a potential role for extrasynaptic NMDA receptors in mutant LRRK2 neurotoxicity.

In addition, increased calcium flux due to increased glutamatergic excitability could impact several other pathological processes ascribed to mutant LRRK2 expression. Mitochondrial perturbations have recently been implicated in mutant LRRK2-associated toxicity. Mitochondrial calcium overload in cortical neurons expressing either G2019S or R1441C LRRK2 leads to enhanced dendritic mitophagy [15]. This loss of mitochondrial density precedes dendritic retraction, and calcium chelators are able to prevent the changes in mitochondrial membrane potential, mitophagy and dendrite shortening elicited by mutant LRRK2. Mitophagy is dependent upon mitochondrial fission, and LRRK2 can interact with DLP1/DRP1 to promote mitochondrial fragmentation in neuronal cells and neurons [14]. Interestingly, calcium dependent phosphatases are involved in activating DLP1/DRP1 function [35], and disrupted calcium homeostasis contributes to autophagy induction by LRRK2 [36]. It is important to keep in mind, however, that while autophagy promotes dendrite retraction, this process could be initiated as a compensatory response to eliminate excessive afferent glutamatergic inputs.

Perturbation in cytoskeletal dynamics is another mechanism linked to LRRK2-mediated neuritic pathology. LRRK2 has been reported to interact with microtubules and to regulate actin remodeling [21, 37]. Enhanced ezrin/radixin/moesin (ERM) protein phosphorylation and blunting of early neurite outgrowth with G2019S LRRK2 expression have been observed in immature (DIV 2) cultured neurons [6]. This inhibition of neurite outgrowth with enhanced pERM-positive filopodia in immature G2019S LRRK2 expressing neurons [6, 19] may reflect commencement of synaptogenesis in lieu of neurite field expansion. In contrast, mutant LRRK2-induced dendrite shortening in pre-differentiated SH-SY5Y cells and in more mature (DIV 14–23) neuron cultures involves autophagy [11, 13, 15], and can be significantly ameliorated by an NMDA antagonist (Fig. 4).

The roles of LRRK2 kinase and GTPase domains in PD pathogenesis are incompletely understood. The G2019S mutation we employed in these studies resides in the kinase domain activation loop and confers an increase in kinase activity over WT LRRK2 [19, 38–43]. We observed increases in synaptic activity and protein immunoreactivity with G2019S LRRK2 expression that were not seen with expression of the kinase impaired K1906M LRRK2, suggesting a role for LRRK2 kinase activity in the regulation of excitatory synapses. Similar effects were also observed with the pathogenic R1441C LRRK2 mutation, which is characterized by decreased GTPase activity [44, 45] with inconsistent effects on in vitro kinase activity (reviewed in [43]). While the relationship between GTPase and kinase activities remain to be fully defined, preserved kinase activity is generally required for LRRK2-associated toxicity [38, 41].

Similar to several reports in the literature demonstrating intermediate effects of WT LRRK2 overexpression [4, 7, 11, 41], we found that transfection with WT LRRK2 often elicited non-significant trends. These trends may be due to lesser increases in cellular LRRK2 kinase activity with WT LRRK2 overexpression, or to the presence of physiological feedback mechanisms that regulate WT LRRK2 but not mutant forms of LRRK2. Transfected primary neuron cultures exhibited equivalent LRRK2 mRNA expression among the WT, G2019S, R1441C and K1906M LRRK2 constructs, and the four LRRK2 constructs elicited equivalent protein expression levels in neuroblastoma cells (Supplementary Fig. 1). Thus, the effects elicited by the disease-associated G2019S and R1441C mutations are unlikely to be due simply to enhanced protein expression or stability [46].

Interestingly, LRRK2 can interact with Parkin, an E3 ubiquitin ligase that is mutated in PARK2-linked autosomal recessive juvenile parkinsonism [4]. When post-synaptically expressed, Parkin dampens excitatory synaptic transmission by pruning excitatory synapses in cultured hippocampal neurons [47]. Thus, either loss of Parkin function or expression of dominant LRRK2 mutations in the post-synaptic compartment elicit increased numbers of excitatory synapses, contributing to enhanced vulnerability to excitotoxicity. Additional putative LRRK2 regulatory targets relevant to excitatory synapse regulation include mRNA translation [22] and mRNA degradation machineries [48], microtubules [18, 22, 49], cell membrane-associated synaptic proteins [50] and Rho GTPases [21].

Excitatory synapse dysregulation is an emerging theme in genetic models of PD. Altered presynaptic vesicle recycling has been observed in cultured cortical neurons with LRRK2

overexpression [24, 51], or with LRRK2 knockdown in presynaptic neurons of connected pairs [23]. Lee and colleagues [22] described distinct LRRK2 mechanisms that impact both pre- and postsynaptic functions in mutant *Drosophila*. Recent work by Parisiadou and colleagues [52] highlight an interaction between LRRK2 and the regulatory subunit IIb of PKA to maintain the PKA holoenzyme in dendritic shafts of striatal projection neurons, reducing PKA in spines. They showed that the R1441C LRRK2 mutation impaired its interaction with PKA, resulting in increased phospho-cofilin and increased synaptic phospho-GluR1. These changes would be expected to stabilize synapses, consistent with our observations. Interestingly, our data implicate a role for LRRK2 kinase activity in excitatory synapse dysregulation, whereas the G2019S mutation did not affect the LRRK2-PKA interaction, suggesting that multiple downstream effector pathways may contribute to the effects of LRRK2 mutations on synaptic dysregulation. Our study is the first to describe alterations in synaptic activity following mutant LRRK2 overexpression in the postsynaptic compartment of mammalian neurons. Furthermore, our data implicate endogenous NMDA receptor activation as a contributing factor in mutant LRRK2 induced dendrite degeneration.

Supplementary Material

Refer to Web version on PubMed Central for supplementary material.

Acknowledgments

This work was supported by the National Institutes of Health [grant numbers R01AG026389 and R01NS065789 to CTC, R01MH045817 to JWJ and R21NS074056 to JWJ]. EDP was supported by NINDS T32 NS07391 Training Grant in Neurobiology of Neurodegenerative Disease and in part by the University of Pittsburgh Pathologist Investigator Residency-Research Training Program (PIRRT). The funders had no role in the study design, data collection and analysis, decision to publish or preparation of the manuscript.

Abbreviations

LRRK2	leucine rich repeat kinase 2
LRRK2-3HA	C-terminal 3x-hemagluttinin tagged LRRK2
cDNA	complementary deoxyribonucleic acid
mEPSC	miniature excitatory postsynaptic current
PD	Parkinson’s disease
AMPA	2-amino-3-(5-methyl-3-oxo-1,2-oxazol-4-yl) propanoic acid)
NMDA	*N*-methyl-D-aspartate
VGLUT1	vesicular glutamate transporter 1
PSD-95	postsynaptic density protein – 95
GFP	green fluorescent protein
WT	wild type
BAC	bacterial artificial chromosome
CNQX	(6-cyano-7-nitroquinoxaline-2,3-dione)

APV	(2*R*)-amino-5-phosphonovaleric acid
CC3	cleaved caspase 3
DAPI	4’,6-diamidino-2-phenylindole
SEM	standard error of the mean
DIV	days *in vitro*

References

1. Paisan-Ruiz C, Jain S, Evans EW, Gilks WP, Simon J, van der Brug M, Lopez de Munain A, Aparicio S, Gil AM, Khan N, Johnson J, Martinez JR, Nicholl D, Carrera IM, Pena AS, Silva Rde, Lees A, Marti-Masso JF, Perez-Tur J, Wood NW, Singleton AB. Cloning of the gene containing mutations that cause PARK8-linked Parkinson’s disease. Neuron. 2004; 44:595–600. [PubMed: 15541308]
2. Zimprich A, Biskup S, Leitner P, Lichtner P, Farrer M, Lincoln S, Kachergus J, Hulihan M, Uitti RJ, Calne DB, Stoessl AJ, Pfeiffer RF, Patenge N, Carbajal IC, Vieregge P, Asmus F, Muller-Myhsok B, Dickson DW, Meitinger T, Strom TM, Wszolek ZK, Gasser T. Mutations in LRRK2 cause autosomal-dominant parkinsonism with pleomorphic pathology. Neuron. 2004; 44:601–607. [PubMed: 15541309]
3. Taymans JM, Cookson MR. Mechanisms in dominant parkinsonism: The toxic triangle of LRRK2, alpha-synuclein, and tau. Bioessays. 2010; 32:227–235. [PubMed: 20127702]
4. Smith WW, Pei Z, Jiang H, Moore DJ, Liang Y, West AB, Dawson VL, Dawson TM, Ross CA. Leucine-rich repeat kinase 2 (LRRK2) interacts with parkin, and mutant LRRK2 induces neuronal degeneration. Proceedings of the National Academy of Sciences of the United States of America. 2005; 102:18676–18681. [PubMed: 16352719]
5. Dachsel JC, Behrouz B, Yue M, Beevers JE, Melrose HL, Farrer MJ. A comparative study of Lrrk2 function in primary neuronal cultures. Parkinsonism & related disorders. 2010; 16:650–655. [PubMed: 20850369]
6. Parisiadou L, Xie C, Cho HJ, Lin X, Gu XL, Long CX, Lobbestael E, Baekelandt V, Taymans JM, Sun L, Cai H. Phosphorylation of ezrin/radixin/moesin proteins by LRRK2 promotes the rearrangement of actin cytoskeleton in neuronal morphogenesis. J Neurosci. 2009; 29:13971–13980. [PubMed: 19890007]
7. Macleod D, Dowman J, Hammond R, Leete T, Inoue K, Abeliovich A. The Familial Parkinsonism Gene LRRK2 Regulates Neurite Process Morphology. Neuron. 2006; 52:587–593. [PubMed: 17114044]
8. Tong Y, Pisani A, Martella G, Karouani M, Yamaguchi H, Pothos EN, Shen J. R1441C mutation in LRRK2 impairs dopaminergic neurotransmission in mice. Proc Natl Acad Sci U S A. 2009; 106:14622–14627. [PubMed: 19667187]
9. Li Y, Liu W, Oo TF, Wang L, Tang Y, Jackson-Lewis V, Zhou C, Geghman K, Bogdanov M, Przedborski S, Beal MF, Burke RE, Li C. Mutant LRRK2(R1441G) BAC transgenic mice recapitulate cardinal features of Parkinson’s disease. Nature neuroscience. 2009; 12:826–828.
10. Ramonet D, Daher JP, Lin BM, Stafa K, Kim J, Banerjee R, Westerlund M, Pletnikova O, Glauser L, Yang L, Liu Y, Swing DA, Beal MF, Troncoso JC, McCaffery JM, Jenkins NA, Copeland NG, Galter D, Thomas B, Lee MK, Dawson TM, Dawson VL, Moore DJ. Dopaminergic Neuronal Loss, Reduced Neurite Complexity and Autophagic Abnormalities in Transgenic Mice Expressing G2019S Mutant LRRK2. PLoS ONE. 2011; 6:e18568. [PubMed: 21494637]
11. Plowey ED, Cherra SJ 3rd, Liu YJ, Chu CT. Role of autophagy in G2019S-LRRK2-associated neurite shortening in differentiated SH-SY5Y cells. Journal of neurochemistry. 2008; 105:1048–1056. [PubMed: 18182054]
12. Alegre-Abarrategui J, Christian H, Lufino MM, Mutihac R, Venda LL, Ansorge O, Wade-Martins R. LRRK2 regulates autophagic activity and localizes to specific membrane microdomains in a

novel human genomic reporter cellular model. Human molecular genetics. 2009; 18:4022–4034. [PubMed: 19640926]

13. Cherra SJ 3rd, Kulich SM, Uechi G, Balasubramani M, Mountzouris J, Day BW, Chu CT. Regulation of the autophagy protein LC3 by phosphorylation. J Cell Biol. 2010; 190:533–539. [PubMed: 20713600]
14. Wang X, Yan MH, Fujioka H, Liu J, Wilson-Delfosse A, Chen SG, Perry G, Casadesus G, Zhu X. LRRK2 regulates mitochondrial dynamics and function through direct interaction with DLP1. Human molecular genetics. 2012; 21:1931–1944. [PubMed: 22228096]
15. Cherra SJ 3rd, Steer E, Gusdon AM, Kiselyov K, Chu CT. Mutant LRRK2 Elicits Calcium Imbalance and Depletion of Dendritic Mitochondria in Neurons. The American journal of pathology. 2013; 182:474–484. [PubMed: 23231918]
16. Papkovskaia TD, Chau KY, Inesta-Vaquera F, Papkovsky DB, Healy DG, Nishio K, Staddon J, Duchen MR, Hardy J, Schapira AH, Cooper JM. G2019S leucine-rich repeat kinase 2 causes uncoupling protein-mediated mitochondrial depolarization. Human molecular genetics. 2012; 21:4201–4213. [PubMed: 22736029]
17. Lichtenberg M, Mansilla A, Zecchini VR, Fleming A, Rubinsztein DC. The Parkinson's disease protein LRRK2 impairs proteasome substrate clearance without affecting proteasome catalytic activity. Cell death & disease. 2:e196.
18. Gillardon F. Interaction of elongation factor 1-alpha with leucine-rich repeat kinase 2 impairs kinase activity and microtubule bundling in vitro. Neuroscience. 2009; 163:533–539. [PubMed: 19559761]
19. Jaleel M, Nichols RJ, Deak M, Campbell DG, Gillardon F, Knebel A, Alessi DR. LRRK2 phosphorylates moesin at threonine-558: characterization of how Parkinson's disease mutants affect kinase activity. The Biochemical journal. 2007; 405:307–317. [PubMed: 17447891]
20. Ho CC, Rideout HJ, Ribe E, Troy CM, Dauer WT. The Parkinson disease protein leucine-rich repeat kinase 2 transduces death signals via Fas-associated protein with death domain and caspase-8 in a cellular model of neurodegeneration. J Neurosci. 2009; 29:1011–1016. [PubMed: 19176810]
21. Chan D, Citro A, Cordy JM, Shen GC, Wolozin B. Rac1 protein rescues neurite retraction caused by G2019S leucine-rich repeat kinase 2 (LRRK2). The Journal of biological chemistry. 2011; 286:16140–16149. [PubMed: 21454543]
22. Lee S, Liu HP, Lin WY, Guo H, Lu B. LRRK2 kinase regulates synaptic morphology through distinct substrates at the presynaptic and postsynaptic compartments of the Drosophila neuromuscular junction. J Neurosci. 2010; 30:16959–16969. [PubMed: 21159966]
23. Piccoli G, Condliffe SB, Bauer M, Giesert F, Boldt K, Astis SDe, Meixner A, Sarioglu H, Vogt-Weisenhorn DM, Wurst W, Gloeckner CJ, Matteoli M, Sala C, Ueffing M. LRRK2 controls synaptic vesicle storage and mobilization within the recycling pool. J Neurosci. 2011; 31:2225–2237. [PubMed: 21307259]
24. Xiong Y, Coombes CE, Kilaru A, Li X, Gitler AD, Bowers WJ, Dawson VL, Dawson TM, Moore DJ. GTPase activity plays a key role in the pathobiology of LRRK2. PLoS Genet. 2010; 6:e1000902. [PubMed: 20386743]
25. Matta S, Kolen KVan, Cunha Rda, van den Bogaart G, Mandemakers W, Miskiewicz K, Bock PJDe, Morais VA, Vilain S, Haddad D, Delbroek L, Swerts J, Chavez-Gutierrez L, Esposito G, Daneels G, Karran E, Holt M, Gevaert K, Moechars DW, Strooper BDe, Verstreken P. LRRK2 controls an EndoA phosphorylation cycle in synaptic endocytosis. Neuron. 2012; 75:1008–1021. [PubMed: 22998870]
26. Qian A, Antonov SM, Johnson JW. Modulation by permeant ions of Mg(2+) inhibition of NMDA-activated whole-cell currents in rat cortical neurons. The Journal of physiology. 2002; 538:65–77. [PubMed: 11773317]
27. Chu CT, Plowey ED, Dagda RK, Hickey RW, Cherra SJ 3rd, Clark RS. Autophagy in neurite injury and neurodegeneration: in vitro and in vivo models. Methods in enzymology. 2009; 453:217–249. [PubMed: 19216909]

28. Meijering E, Jacob M, Sarria JC, Steiner P, Hirling H, Unser M. Design and validation of a tool for neurite tracing and analysis in fluorescence microscopy images. Cytometry A. 2004; 58:167–176. [PubMed: 15057970]
29. Kim MJ, Dunah AW, Wang YT, Sheng M. Differential roles of NR2A- and NR2B-containing NMDA receptors in Ras-ERK signaling and AMPA receptor trafficking. Neuron. 2005; 46:745–760. [PubMed: 15924861]
30. Ivanov A, Pellegrino C, Rama S, Dumalska I, Salyha Y, Ben-Ari Y, Medina I. Opposing role of synaptic and extrasynaptic NMDA receptors in regulation of the extracellular signal-regulated kinases (ERK) activity in cultured rat hippocampal neurons. The Journal of physiology. 2006; 572:789–798. [PubMed: 16513670]
31. Wroge CM, Hogins J, Eisenman L, Mennerick S. Synaptic NMDA receptors mediate hypoxic excitotoxic death. J Neurosci. 2012; 32:6732–6742. [PubMed: 22573696]
32. Hardingham GE, Fukunaga Y, Bading H. Extrasynaptic NMDARs oppose synaptic NMDARs by triggering CREB shut-off and cell death pathways. Nature neuroscience. 2002; 5:405–414.
33. Hardingham GE, Bading H. Synaptic versus extrasynaptic NMDA receptor signalling: implications for neurodegenerative disorders. Nature reviews. 2010; 11:682–696.
34. Xia P, Chen HS, Zhang D, Lipton SA. Memantine preferentially blocks extrasynaptic over synaptic NMDA receptor currents in hippocampal autapses. J Neurosci. 2010; 30:11246–11250. [PubMed: 20720132]
35. Cribbs JT, Strack S. Reversible phosphorylation of Drp1 by cyclic AMP-dependent protein kinase and calcineurin regulates mitochondrial fission and cell death. EMBO reports. 2007; 8:939–944. [PubMed: 17721437]
36. Gomez-Suaga P, Luzon-Toro B, Churamani D, Zhang L, Bloor-Young D, Patel S, Woodman PG, Churchill GC, Hilfiker S. Leucine-rich repeat kinase 2 regulates autophagy through a calcium-dependent pathway involving NAADP. Human molecular genetics. 2012; 21:511–525. [PubMed: 22012985]
37. Gandhi PN, Wang X, Zhu X, Chen SG, Wilson-Delfosse AL. The Roc domain of leucine-rich repeat kinase 2 is sufficient for interaction with microtubules. Journal of neuroscience research. 2008; 86:1711–1720. [PubMed: 18214993]
38. Greggio E, Jain S, Kingsbury A, Bandopadhyay R, Lewis P, Kaganovich A, van der Brug MP, Beilina A, Blackinton J, Thomas KJ, Ahmad R, Miller DW, Kesavapany S, Singleton A, Lees A, Harvey RJ, Harvey K, Cookson MR. Kinase activity is required for the toxic effects of mutant LRRK2/dardarin. Neurobiology of disease. 2006; 23:329–341. [PubMed: 16750377]
39. West AB, Moore DJ, Choi C, Andrabi SA, Li X, Dikeman D, Biskup S, Zhang Z, Lim KL, Dawson VL, Dawson TM. Parkinson's disease-associated mutations in LRRK2 link enhanced GTP-binding and kinase activities to neuronal toxicity. Human molecular genetics. 2007; 16:223–232. [PubMed: 17200152]
40. Luzon-Toro B, de la Torre ER, Delgado A, Perez-Tur J, Hilfiker S. Mechanistic insight into the dominant mode of the Parkinson's disease-associated G2019S LRRK2 mutation. Human molecular genetics. 2007
41. Smith WW, Pei Z, Jiang H, Dawson VL, Dawson TM, Ross CA. Kinase activity of mutant LRRK2 mediates neuronal toxicity. Nature neuroscience. 2006; 9:1231–1233.
42. West AB, Moore DJ, Biskup S, Bugayenko A, Smith WW, Ross CA, Dawson VL, Dawson TM. Parkinson's disease-associated mutations in leucine-rich repeat kinase 2 augment kinase activity. Proceedings of the National Academy of Sciences of the United States of America. 2005; 102:16842–16847. [PubMed: 16269541]
43. Greggio E, Cookson MR. Leucine-rich repeat kinase 2 mutations and Parkinson's disease: three questions. ASN neuro. 2009; 1
44. Lewis PA, Greggio E, Beilina A, Jain S, Baker A, Cookson MR. The R1441C mutation of LRRK2 disrupts GTP hydrolysis. Biochemical and biophysical research communications. 2007; 357:668–671. [PubMed: 17442267]
45. Guo L, Gandhi PN, Wang W, Petersen RB, Wilson-Delfosse AL, Chen SG. The Parkinson's disease-associated protein, leucine-rich repeat kinase 2 (LRRK2), is an authentic GTPase thatstimulates kinase activity. Experimental cell research. 2007

46. Herzig MC, Kolly C, Persohn E, Theil D, Schweizer T, Hafner T, Stemmelen C, Troxler TJ, Schmid P, Danner S, Schnell CR, Mueller M, Kinzel B, Grevot A, Bolognani F, Stirn M, Kuhn RR, Kaupmann K, van der Putten PH, Rovelli G, Shimshek DR. LRRK2 protein levels are determined by kinase function and are crucial for kidney and lung homeostasis in mice. Human molecular genetics. 2011; 20:4209–4223. [PubMed: 21828077]

47. Helton TD, Otsuka T, Lee MC, Mu Y, Ehlers MD. Pruning and loss of excitatory synapses by the parkin ubiquitin ligase. Proceedings of the National Academy of Sciences of the United States of America. 2008; 105:19492–19497. [PubMed: 19033459]

48. Gehrke S, Imai Y, Sokol N, Lu B. Pathogenic LRRK2 negatively regulates microRNA-mediated translational repression. Nature. 2010; 466:637–641. [PubMed: 20671708]

49. Lin X, Parisiadou L, Gu XL, Wang L, Shim H, Sun L, Xie C, Long CX, Yang WJ, Ding J, Chen ZZ, Gallant PE, Tao-Cheng JH, Rudow G, Troncoso JC, Liu Z, Li Z, Cai H. Leucine-rich repeat kinase 2 regulates the progression of neuropathology induced by Parkinson's-disease-related mutant alpha-synuclein. Neuron. 2009; 64:807–827. [PubMed: 20064389]

50. Berger Z, Smith KA, Lavoie MJ. Membrane localization of LRRK2 is associated with increased formation of the highly active LRRK2 dimer and changes in its phosphorylation. Biochemistry. 2010; 49:5511–5523. [PubMed: 20515039]

51. Shin N, Jeong H, Kwon J, Heo HY, Kwon JJ, Yun HJ, Kim CH, Han BS, Tong Y, Shen J, Hatano T, Hattori N, Kim KS, Chang S, Seol W. LRRK2 regulates synaptic vesicle endocytosis. Exp Cell Res. 2008; 314:2055–2065. [PubMed: 18445495]

52. Parisiadou L, Yu J, Sgobio C, Xie C, Liu G, Sun L, Gu XL, Lin X, Crowley NA, Lovinger DM, Cai H. LRRK2 regulates synaptogenesis and dopamine receptor activation through modulation of PKA activity. Nature neuroscience. 2014; 17:367–376.

Highlights

- Neurons expressing mutant LRRK2 exhibit increased glutamatergic excitability
- G2019S or R1441C, but not kinase dead, LRRK2 increases excitatory synapse density
- The NMDA antagonist memantine reduces mutant LRRK2-induced dendrite retraction
- Increased calcium may function upstream of other known effects of mutant LRRK2
- Synaptic dysfunction represents an early feature of mutant LRRK2 toxicity

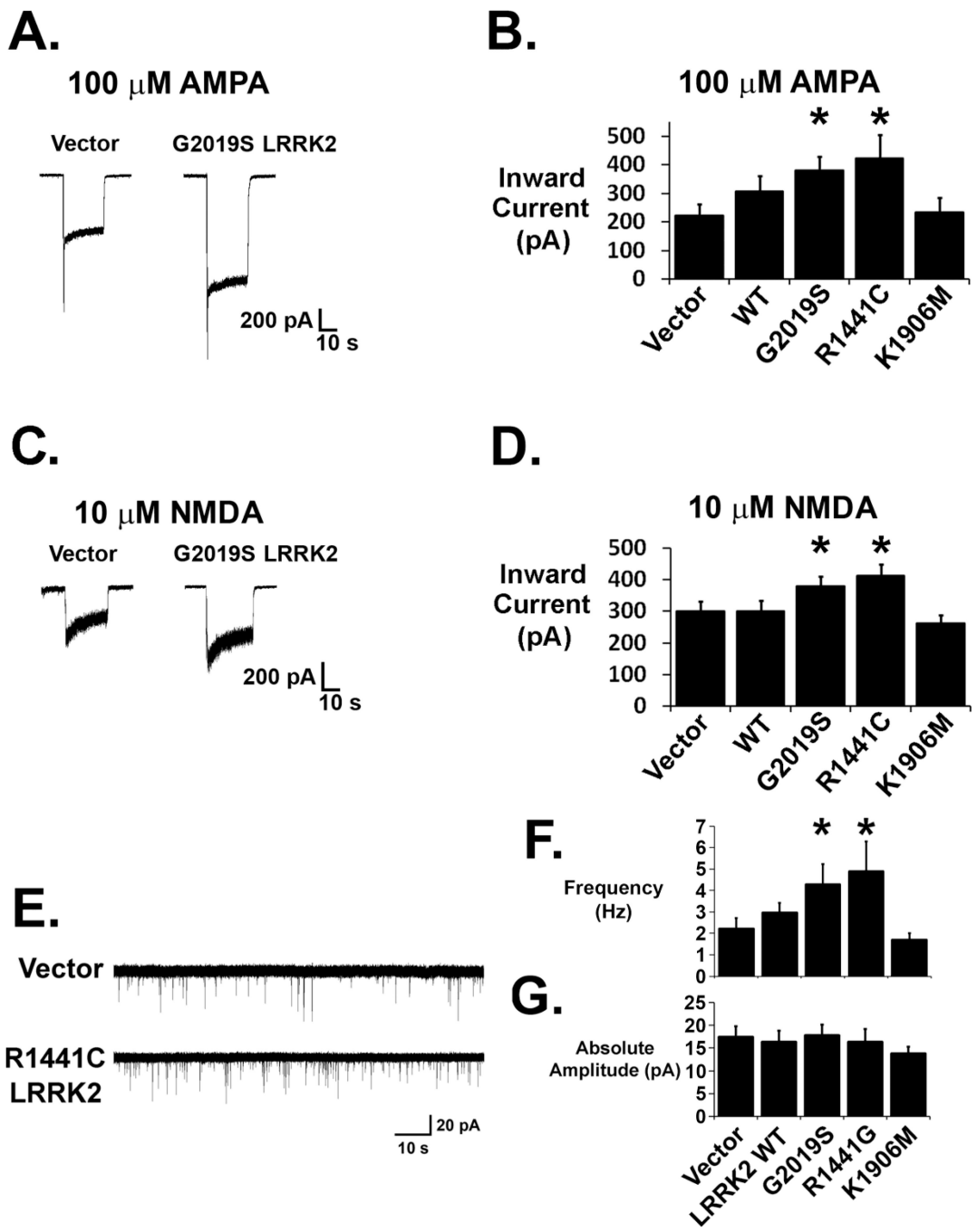

Figure 1. Whole-cell current responses to glutamate receptor agonists and mEPSC activity are increased in LRRK2 transfected neurons

(A, B) Steady state inward current responses to 100 μM AMPA at a holding potential of −55 mV were significantly larger in G2019S- and R1441C-expressing neurons, but not in K1906M-expressing neurons (* $p<0.05$ compared to vector-transfected neurons, ANOVA: 4 df, F-Ratio: 2.552; $n_{Vector} = 24$; $n_{WT} = 18$; $n_{G2019S} = 27$; $n_{R1441C} = 18$; $n_{1906M} = 14$). WT LRRK2-transfected neurons showed a trend towards increased AMPA responses. (C, D) Steady state inward current responses to 10 μM NMDA were significantly larger in G2019S and R1441C LRRK2 overexpressing neurons (* $p<0.05$ compared to vector-transfected

neurons, ANOVA: 4 df, F-Ratio: 3.996) but were unaltered with overexpression of WT or K1906M LRRk2 (E) Raw traces from mEPSC recordings (holding potential −60 mV) showing increased mEPSC events per unit time in a R1441C LRRK2-transfected neuron (bottom) compared to the control vector-transfected neuron (top). (F) Composite data demonstrate increased mean mEPSC frequencies in neurons overexpressing mutant G2019S LRRK2 (n=10; $p<0.05$) or R1441C LRRK2 (n=10; $p<0.05$) and a modest trend towards increased mEPSC frequency in WT LRRK2 (n=14) compared to vector control (n=14) and K1906M LRRK2 (n=8; ANOVA: 4 df, F-Ratio: 2.654). (G) There was no difference in mean mEPSC amplitude among treatment groups (ANOVA: 4 df, F-Ratio: 0.545).

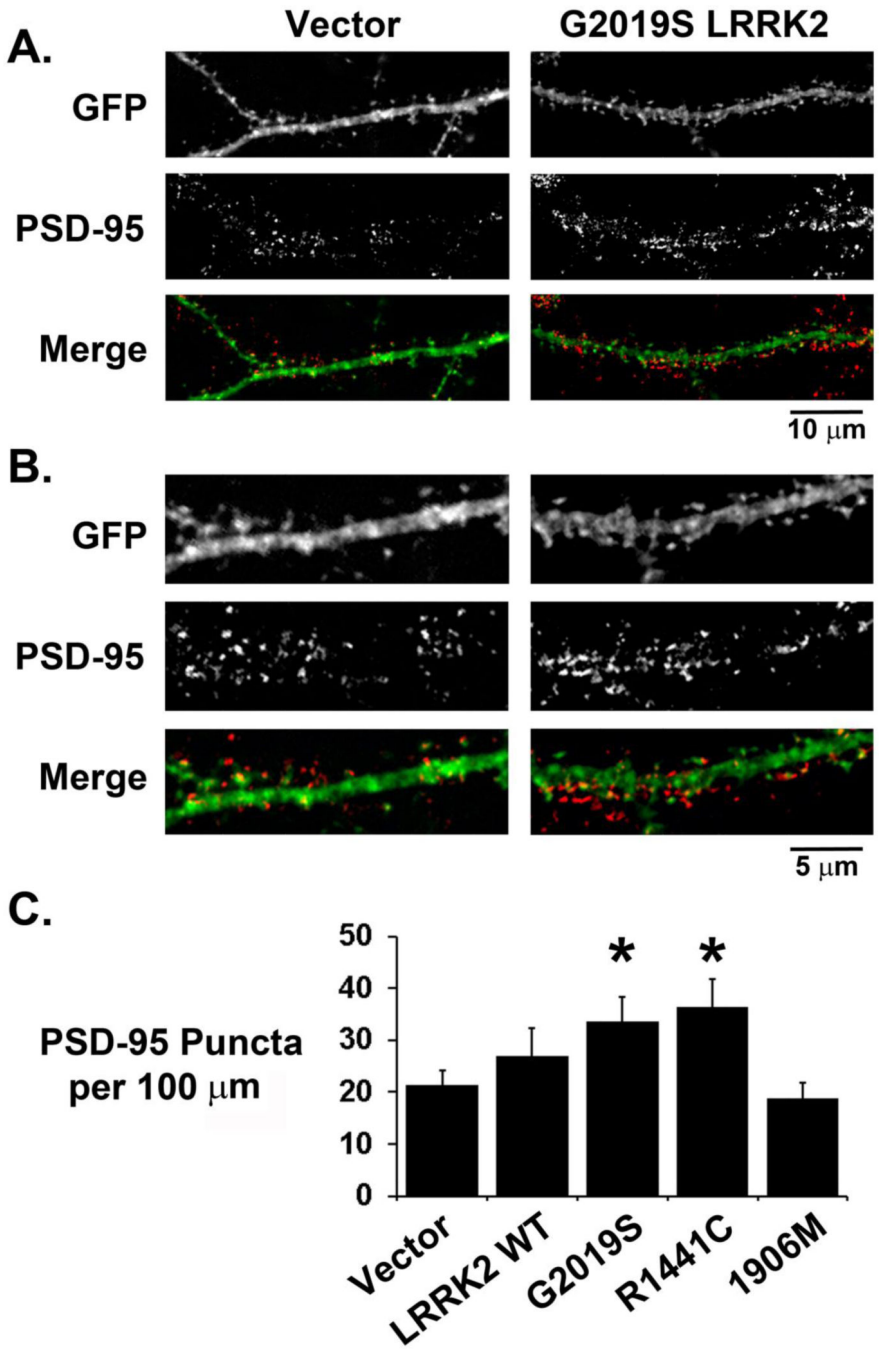

Figure 2. Pathogenic mutant LRRK2-transfected neurons show increased dendritic PSD-95 immunoreactivity

Medium (A) and high (B) power images of GFP/LRRK2 co-transfected neurons immunostained for the glutamatergic postsynaptic marker PSD-95. Many PSD-95 immunoreactive puncta are observed to colocalize with GFP positive dendrites and spines. (C) Composite data showing increased dendritic PSD-95 immunoreactive puncta on dendrites of neurons expressing G2019S LRRK2 (n=26) or R1441C LRRK2 (n=21), but not K1906M LRRK2 (n=25) or WT LRRK2 (* $p<0.05$ compared to control vector dendrites (n=26), ANOVA: 4 df, F-Ratio: 3.371).

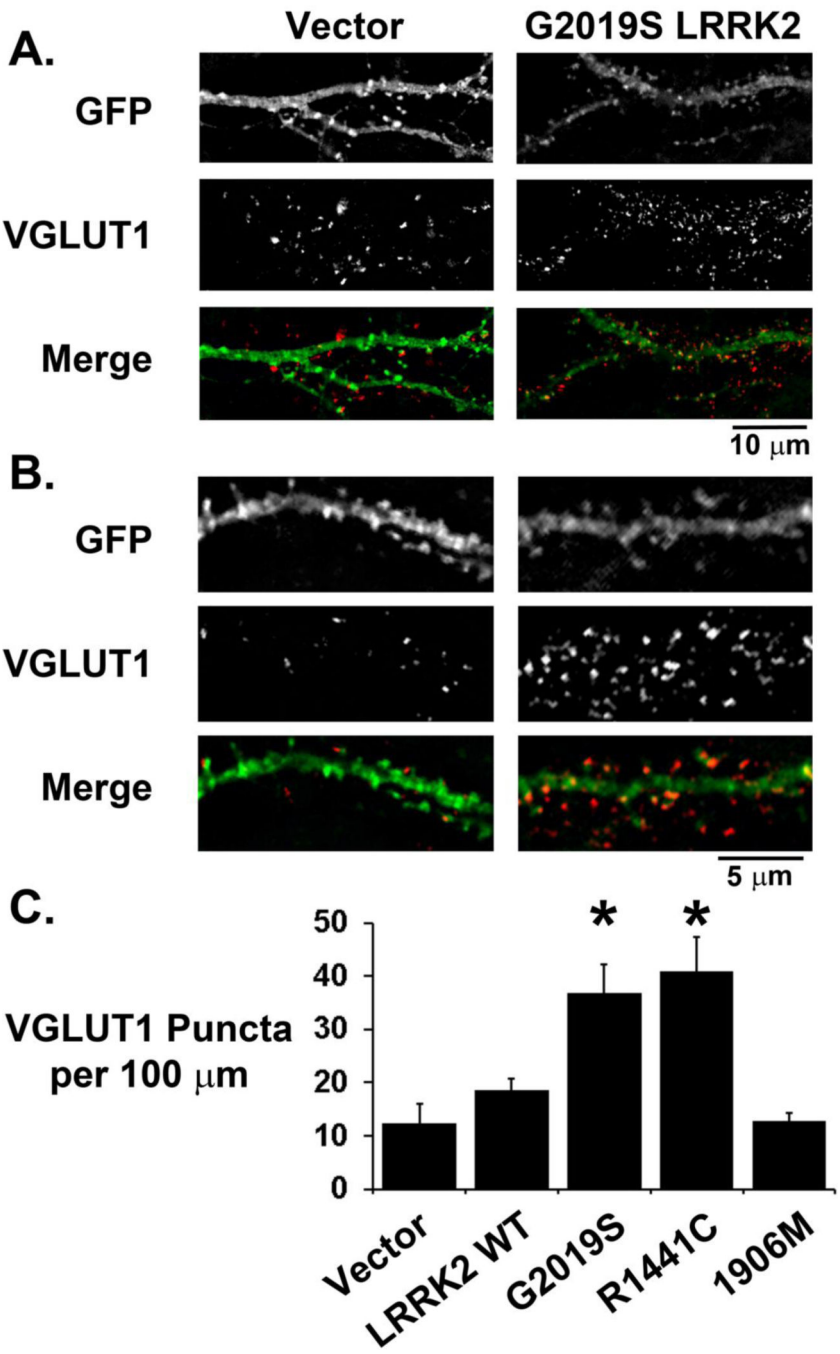

Figure 3. VGLUT1 immunoreactivity is increased around dendrites of mutant LRRK2-expressing neurons

Medium (A) and high (B) power images of GFP/LRRK2 co-transfected neurons immunostained for the glutamatergic presynaptic marker VGLUT1. VGLUT1 immunoreactive puncta are observed to abut and colocalize with GFP positive dendrites and spines. (C) Composite data showing increased dendritic VGLUT1 immunoreactivity around dendrites of G2019S LRRK2 (n=36) and R1441C LRRK2 (n=47) transfected neurons but no significant difference around WT LRRK2 or kinase impaired K1906M LRRK2 transfected

dendrites (n=38) (* $p<0.001$ compared to control vector dendrites (n=35), ANOVA: 4 df, F-Ratio: 10.002).

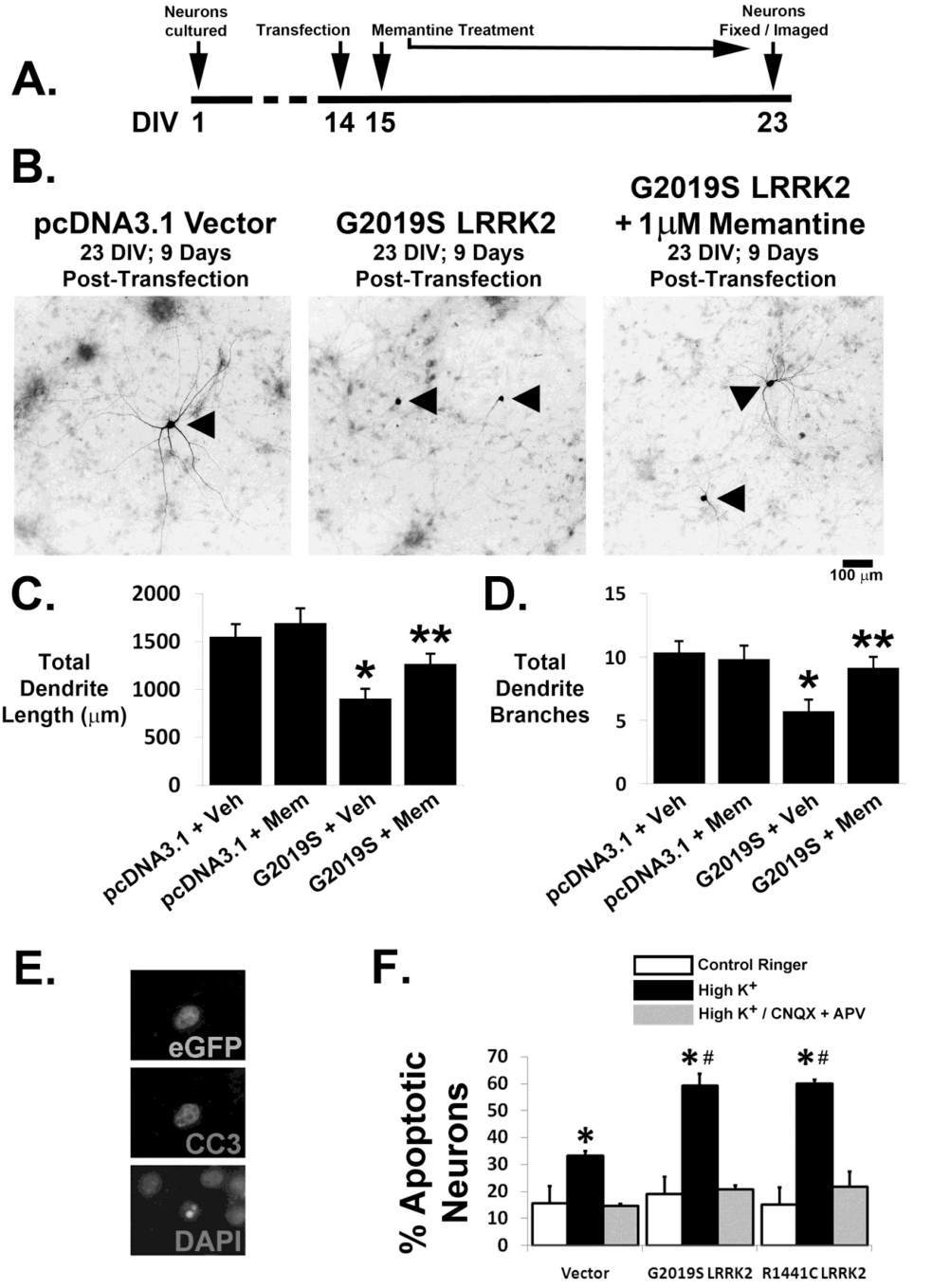

Figure 4. Neurons are partially protected from mutant LRRK2-induced neurodegeneration by the NMDA receptor antagonist memantine and show increased susceptibility to synaptic glutamate stress

(A) Schematic of experimental design depicting continuous treatment of transfected neurons with 1 μM memantine following transfection with vector or G2019S LRRK2. (B) Representative neurons (arrowheads) 9 days following transfection with vector (left panel), G2019S LRRK2 (middle, showing severe blunting of the dendritic arborization) or G2019S LRRK2 with 1μM memantine treatment (right). Compared to vector transfected neurons, G2019S LRRK2 transfected neurons demonstrated dendrite length attenuation (C; * $p<0.05$,

ANOVA: 3 df, F-Ratio: 5.621) and dendritic branching complexity attenuation (D; * $p<0.05$, ANOVA: 3 df, F-Ratio: 5.621), which were significantly reversed by memantine treatment. (E, F) Cortical cultures transfected with either vector or mutant LRRK2 were subjected to 5 minutes of depolarization with high K^+ Ringer (90 mM) in the presence or absence of AMPA and NMDA receptor antagonists (25 μM CNQX and 50 μM D-APV). Following a 12-hour incubation period, cultures were fixed and stained for CC3 (E). Significantly larger proportions of pathogenic mutant LRRK2 expressing neurons demonstrated apoptosis following synaptic glutamate exposure compared to vector transfected neurons (F) (* $p<0.05$ compared to control ringer; # $p<0.05$ compared to vector transfected neurons in high K^+). No significant apoptosis was seen in the presence of the glutamate receptor antagonists.